

The Materials Research Society (MRS)

XXIV INTERNATIONAL MATERIALS

RESEARCH CONGRESS 2015

XIV NACE International Congress-Mexican Section

J.G. Chacón-Nava

Centro de Investigación en Materiales Avanzados, S.C., Departamento de Metalurgia e Integridad Estructural, Miguel de Cervantes 120, Complejo Industrial Chihuahua, Chihuahua, México.
E-mail: jose.chacon@cimav.edu.mx

A. Borunda-Terrazas

Centro de Investigación en Materiales Avanzados, S.C., Departamento de Metalurgia e Integridad Estructural, Miguel de Cervantes 120, Complejo Industrial Chihuahua, Chihuahua, México.

Z. Guzmán-Escobedo

Centro de Investigación en Materiales Avanzados, S.C., Departamento de Metalurgia e Integridad Estructural, Miguel de Cervantes 120, Complejo Industrial Chihuahua, Chihuahua, México.

A. Martínez-Villafañe

Centro de Investigación en Materiales Avanzados, S.C., Departamento de Metalurgia e Integridad Estructural, Miguel de Cervantes 120, Complejo Industrial Chihuahua, Chihuahua, México.

C.G. Nava-Dino

Universidad Autónoma de Chihuahua
Facultad de Ingeniería
Circuito Univ. S/n
Chihuahua, Chih., México.

M. M. Stack

Tribology Research Group
Mechanical and Aerospace Engineering
Strathclyde University
Glasgow, Scotland, UK

EROSION-CORROSION OF 12 CR STEEL AT HIGH TEMPERATURES AND LOW IMPACT VELOCITY

ABSTRACT

Erosion-corrosion by either solid particle or liquid impact remains an issue affecting a wide variety of industries (from coal conversion processes to steam turbines in nuclear power generation). The E-C phenomena depend on properties of the material tested, particle properties and the nature of the environment (impact velocity, temperature and corrosivity). In studies of erosion-corrosion, the effects of alloy corrosion resistance are generally not well understood. The aim of the present work was to undertake a systematic study on the effects of erodent velocity for a 12 Cr stainless steel (taking for comparison a mild steel). Experiments were carried out in a FB rig at temperatures from 300 to 600⁰C and impact velocities between 1.5 and 4.5 m/s. The erodent used was alumina particles. Here, weight change data and analytical scanning electron microscopy were used to characterize materials degradation. The results showed that the ranking order of the wear rates of the alloys varied as a function of temperature and velocity. Reasons to explain the behavior found are given and discussed.

INTRODUCTION

It is known that material wastage of owing to the combined effects of erosion and corrosion may be a major technology limiting problem in a wide range of industrial environments from advanced coal conversion systems, to chemical and petrochemical industries. In many of the process involved, erosion-corrosion occurs by solid particles at elevated temperatures in a wide range of impact velocities. In such environments, wastage is dependent on the properties of a range of variables, among others: particle (velocity, density, hardness, shape, size, corrosiveness), target (hardness, corrosion resistance), (iii) corrosion potential: gas partial pressure, temperature, (iv) impact velocity of particles, or fluid velocity.

Fluidised Bed Combustors (FBC) units can suffer materials deterioration due to particle interaction of solid particles with the heat transfer tubes immersed on the bed (1-3).

The effects of erosion-corrosion variables in FBC environments have lead to the classification of various erosion-corrosion regimes (4). The transitions between such regimes are best understood by considering the effect of temperature, Fig. 1. At low temperatures, erosion of the alloy substrate is the dominant process. As the temperature is increased, the rate of formation of corrosion product increases. If this oxide/scale that forms between successive erosion events is removed after impactation, a temperature is eventually reached where the removal of corrosion product is the dominant wastage mechanism. This is the regime in which corrosion enhances the erosion-corrosion rate, and marks the transition to the "erosion-corrosion dominated" regime. These erosion-corrosion regimes are described as: (i) erosion dominated (corrosion is negligible) , (ii) erosion-corrosion dominated (corrosion enhances erosion), (iii) corrosion-dominated 1 (corrosion inhibits erosion) and (iv) corrosion-dominated 2 (erosion is negligible).

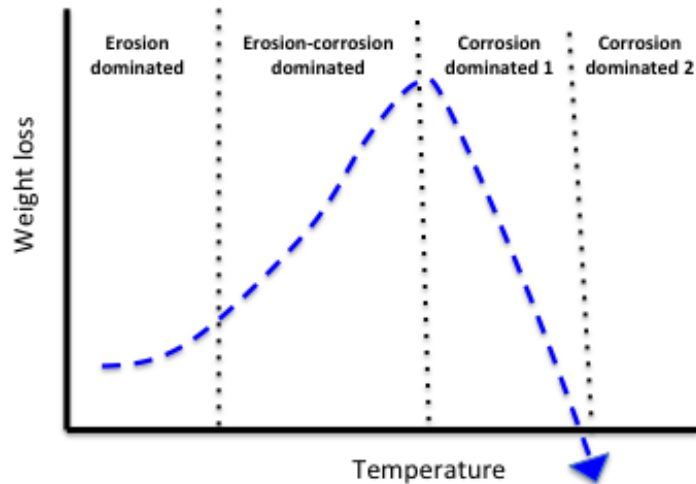


Fig. 1.- Schematic diagram of the transitions through the erosion- corrosion regimes as a function of temperature.

The effects of velocity in solid particle erosion are well established. The generalized relationship which relates erosion to impact velocity is given by:

$$E = K V^n f(\Theta) \dots \dots \dots (1)$$

where E = erosión, k = constant, v = velocity, n = exponent and θ = impact angle.

The velocity exponents which are usually reported for the erosion of metals vary between 2 and 3 (5). In erosion-corrosion, however, the effects of velocity are complicated by the fact that erosion conditions determine the extent of corrosion on the surface.

Although there has been much progress in the understanding of erosion-corrosion in such processes, there are still aspects regarding materials performance that are not well understood. The aim of the present work was to investigate the effect of temperature and impact velocity in laboratory simulated fluidised bed environments of a 12 Cr stainless steel. For comparison purposes, mild steel was chosen.

EXPERIMENTAL PROCEDURES.

The materials tested were two commercial Fe-based alloys: a Fe-12% Cr stainless steel (heated at 750⁰C for 30 min., air cooled) and mild steel (tested in the as-received condition). Table 1 shows the chemical composition (%wt) for the steels. Cylindrical specimens with typical dimensions of about 6 mm diameter and were used. Before exposure, the specimens were ground to a final surface finish with 800 grit SiC paper, rinsed in methanol, and degreased with acetone. The extent of damage to specimens exposed to the erosion rig was determined by the weight loss method using a Sartorius microbalance, with a resolution of 10⁻⁶ g.

In order to estimate the oxide scale thickness formed on both steels after oxidation in air, the gravimetric method was used (6). Oxidation experiments were carried out at different temperatures for 24 h using rectangular specimens of an area of approximately 0.1 mm² and weights of about 10 mg.

Experiments were carried out in a fluidized bed (FB) rig, which basically consist of a) a fluidized-bed chamber containing approximately 40 % vol. of particles during a test, b) a specimen holder system and c) a heating system. Fig 2 shows a general schematic of the apparatus used. This consists of a light fluidized-bed of particles in which cylindrical specimens are rotated in the vertical plane into and out of the bed. Depending upon the angular velocity chosen, the linear velocity of the specimens relative to the particles is achieved.

Relatively angular alumina particles of 560 µm average size were used at impact velocities from 1 m/s to 4.5 m/s. The range of temperature was from 100⁰C up to 600⁰C, using air as oxidant gas. All test last 24 hours. Morphological examinations of specimens surface were carried out using an AMRAY scanning electron microscope, linked with an EDX unit.

Material	12 Cr SS	Mild Steel
C	0.07	0.20
Mn	1.5	0.7
Si	1.0	0.3
P and S	0.03	0.05
Cr	12.50	---
Ni	1.0	---
Mo	0.60	---
Fe	Bal.	Bal.
Hv±10	180	160

Table I. Chemical composition (%wt) and hardness (Hv) of the steels used.

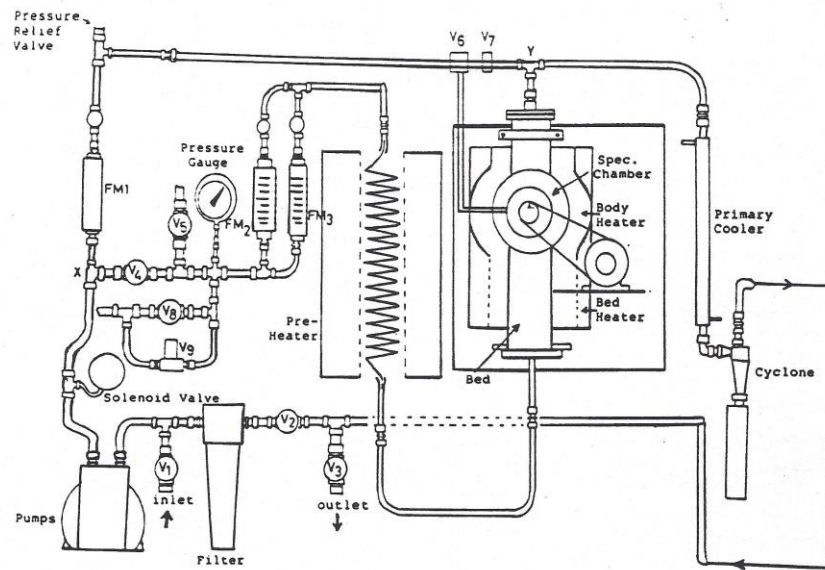


Fig. 2 Schematic diagram of the E-C rig used.

RESULTS AND DISCUSSION.

From the oxidation tests, Table II shows the oxide/film thickness for each steel at the various temperatures.

	300 ⁰ C	450 ⁰ C	500 ⁰ C	600 ⁰ C
12 Cr	0.1 $\mu\text{m}^{(1)}$	0.3 $\mu\text{m}^{(1)}$	n. d.	0.5 $\mu\text{m}^{(1)}$
Mild steel	0.2 $\mu\text{m}^{(1)}$	~ 3 $\mu\text{m}^{(2)}$	~ 6.5 $\mu\text{m}^{(2)}$	~ 17 $\mu\text{m}^{(2)}$

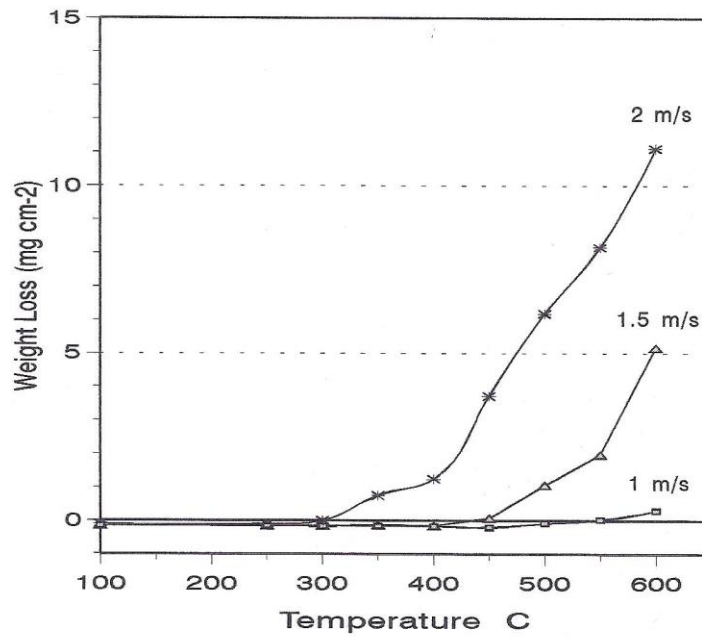
(1)Determined by the gravimetric method

(2)Determined by SEM observation

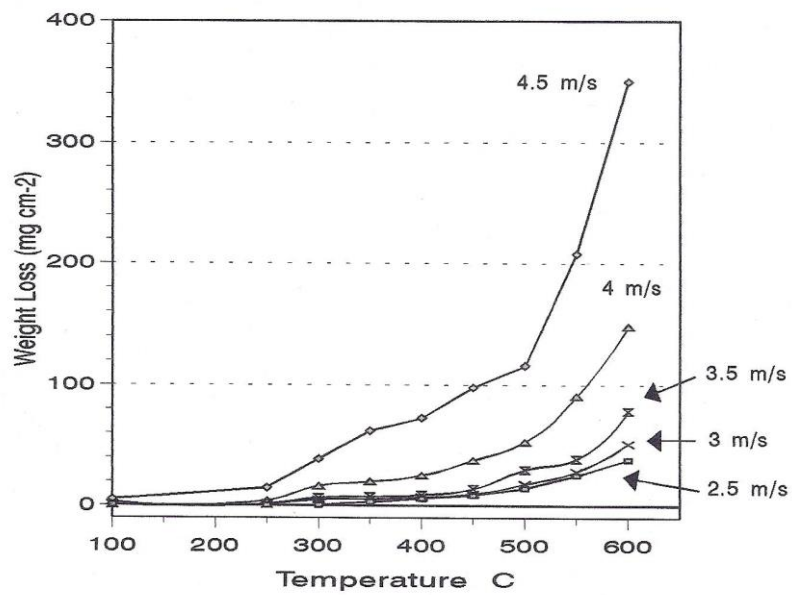
Table II.- Estimated oxide/film thickness values for a 12 CR SS and mild steel after oxidation in still air at different temperatures for 24 h.

Fig. 3 shows that no weight loss peak was recorded, under any condition. The onset of weight loss over all the temperature range was found to be strongly dependent on impact velocity. For example, at 1 m/s no weight loss was recorded at temperatures below 550⁰C, only a small constant weight gain. Increasing velocity reduced quite significantly this threshold temperature. At 2 m/s it fell to 300⁰C, and, at 4.5 m/s it was less than 100⁰C. Above this threshold temperature, the weight loss increased non-linearly with temperature in all cases.

At 100⁰C and below 2.5 m/s no weight losses were observed; above this velocity, the weight loss increased non-linearly to ~ 5 mg/cm². At 300⁰C, a slight increase in weight loss was observed, and, within the velocity range from 2 m/s to 3.5 m/s, little variation in weight loss was found at temperatures up to 400⁰C. Above 3.5 m/s, a rapid increase in wastage was noted. A very similar pattern was found at higher temperatures, the weight loss magnitude being the only obvious difference.



a



b)

Fig. 3 Weight change as a function of temperature and impact velocity for 12 Cr steel exposed in the FB rig with 560 μ m alumina particles for 24 h.

A most distinctive feature of the weight loss of this steel as a function of temperature is that a peak wastage temperature (the so called critical temperature) was not found. Instead, for a given impact velocity, the weight losses recorded increased with increase temperature.

A probable explanation for this could reside in the large alumina particles used in this studies i.e. 560 μm as compared with previous reports from the literature (7). Under impact, at a given velocity, larger particles produce more energetic impact events, which may disrupt and/or remove more easily an oxide film (and/or base metal). Sethi and Corey (8) suggested that, under a given set of conditions, a decrease in the equilibrium film thickness would be expected with increasing particle size.

Hence, higher temperatures are needed to reach the so-called critical oxide thickness, and, in accordance with the results of Sethi and Corey (8) the net effect would be a shift to the right in the transition from this temperature regime in to a corrosion-dominated regime. At the highest temperature, further increase in velocity to 4.5 m s^{-1} could cause a significant increase in oxide film thickness. This might suggest a higher oxidation enhancement due to more energetic impacts but despite this, no transition into a corrosion-dominated regime was observed.

The behaviour of these steels with temperature may be described within the following zones:

Zone I.- Observed at temperatures below 300°C , and velocities below 2.5 m/s .

In general, within this regime, no significant wastage was recorded; instead, small weight gains were observed. Such weight gains cannot be associated with alloy oxidation simply because of the low temperatures. Thus, these weight gains are more likely due to erodent deposition, which seems to be favoured at low temperatures and velocities.

Zone II.- At temperatures from 300⁰C to 600⁰C, and velocities above 1.5 m/s.

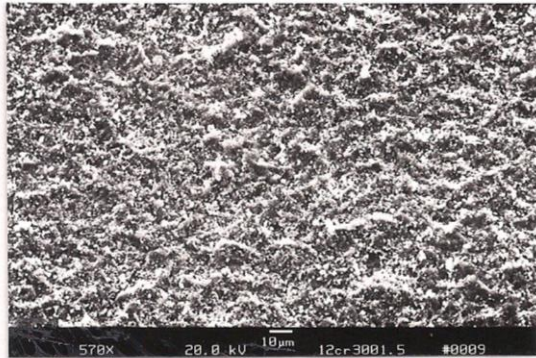
Here, the wastage increased significantly with increasing temperature and velocity. For the 12 Cr steel, its mechanical properties are not severely affected below 600⁰C. Thus, oxidation should played an important role.

Morphologies of the wear scars.

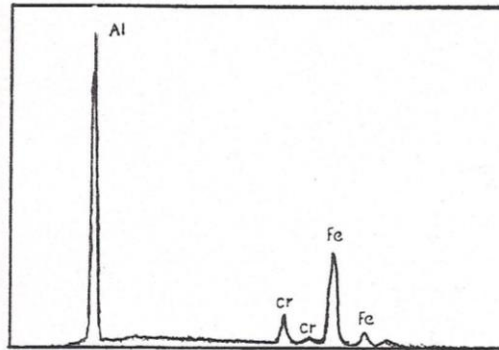
Fig 4(a) shows a rippled surface at 300⁰C and 1.5 m/s, although, at this low velocity, considerable amounts of erodent debris remained on the surface, as indicated by EDX analysis, Fig. 4(b). Increasing the velocity to 4.5 m/s produced a rather different morphology: at low magnification, a roughen surface was observed, but, at higher magnification, wear tracks were apparent, aligned in the direction of particle flow. Typically, the length of these tracks was between 10 and 40 μm, Fig. 4(c). EDX analysis showed dominant iron and chromium peaks, and very weak aluminum peaks, Fig. 4(d).

At 450⁰C and 2.5 m/s ripples were noted again, but, in some discrete areas, spallation of scale was also noted, Fig. 5(a and b). EDX analysis showed a dominant iron peak, although an aluminium peak of low intensity was also detected Fig. 5(c).

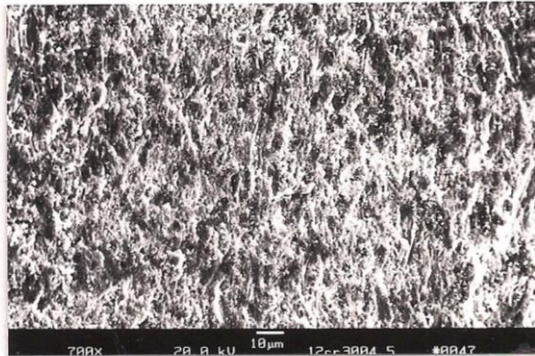
Further increases in temperature and velocity resulted in smooth surfaces and ripples were no longer seen. At 600⁰C, wear tracks of 10 to 20 μm length were observed, in particular at higher magnification, Fig. 6(a and b). Local EDX analysis of the wear scars showed strong peaks for iron, chromium and oxygen, and weak aluminium signals, Fig. 6(c).



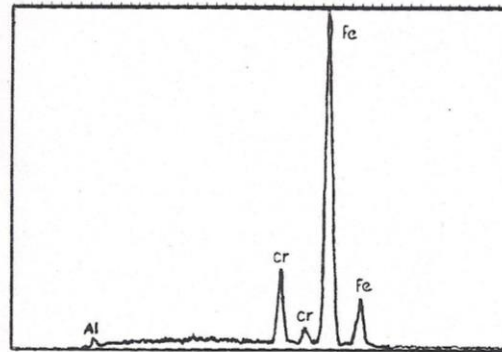
a) 300°C, 1.5 m s⁻¹



b) EDX analysis on surface in a).



c) 300°C, 4.5 m s⁻¹



d) EDX analysis on surface in c).

Fig. 4.- SEM micrographs of the 12 Cr SS exposed in the E-C rig at 300°C with the 560 μm alumina particles at impact velocities of a) 1.5 m/s and c) 4.5 m/s for 24 h; b) and d) show their respective surface EDX analyses.

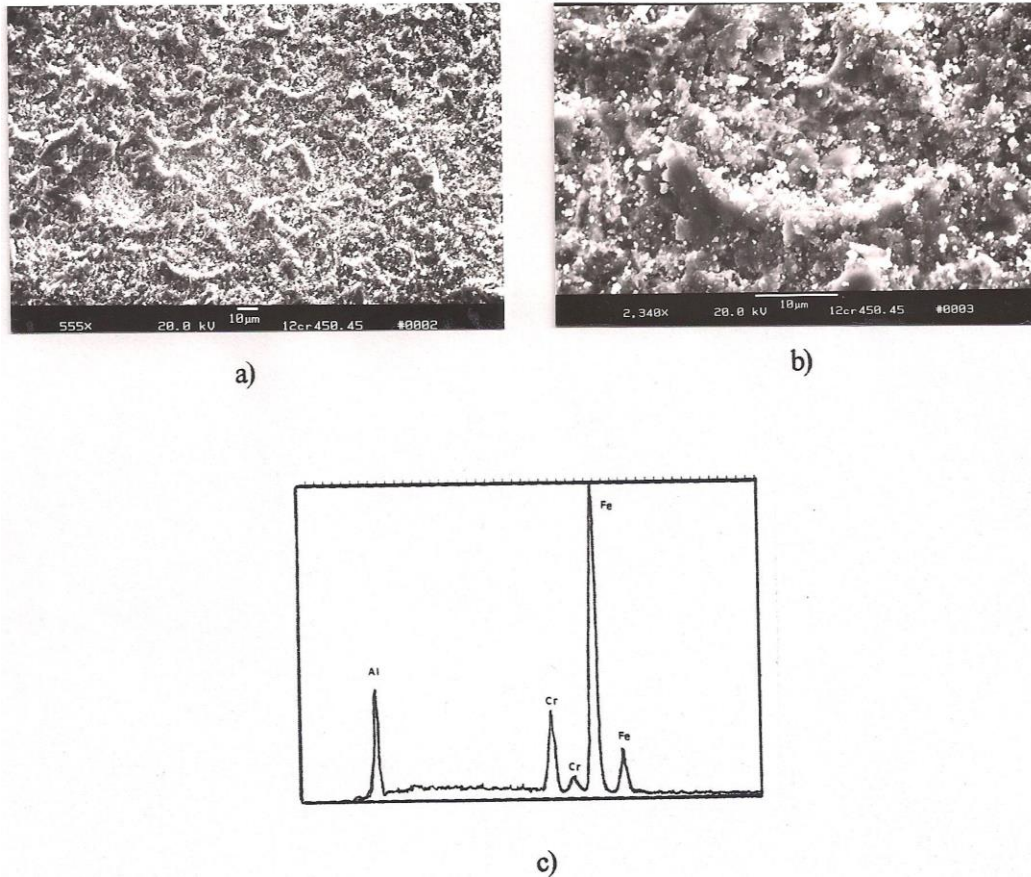


Fig. 5.- SEM micrographs of the 12 Cr SS exposed in the E-C rig at 450⁰C with the 560 μm alumina particles an impact velocity of 2.5 m/s for 24 h; a) surface morphology, b) view at higher magnification showing ripple formation, and c) EDX analysis of the surface in a).

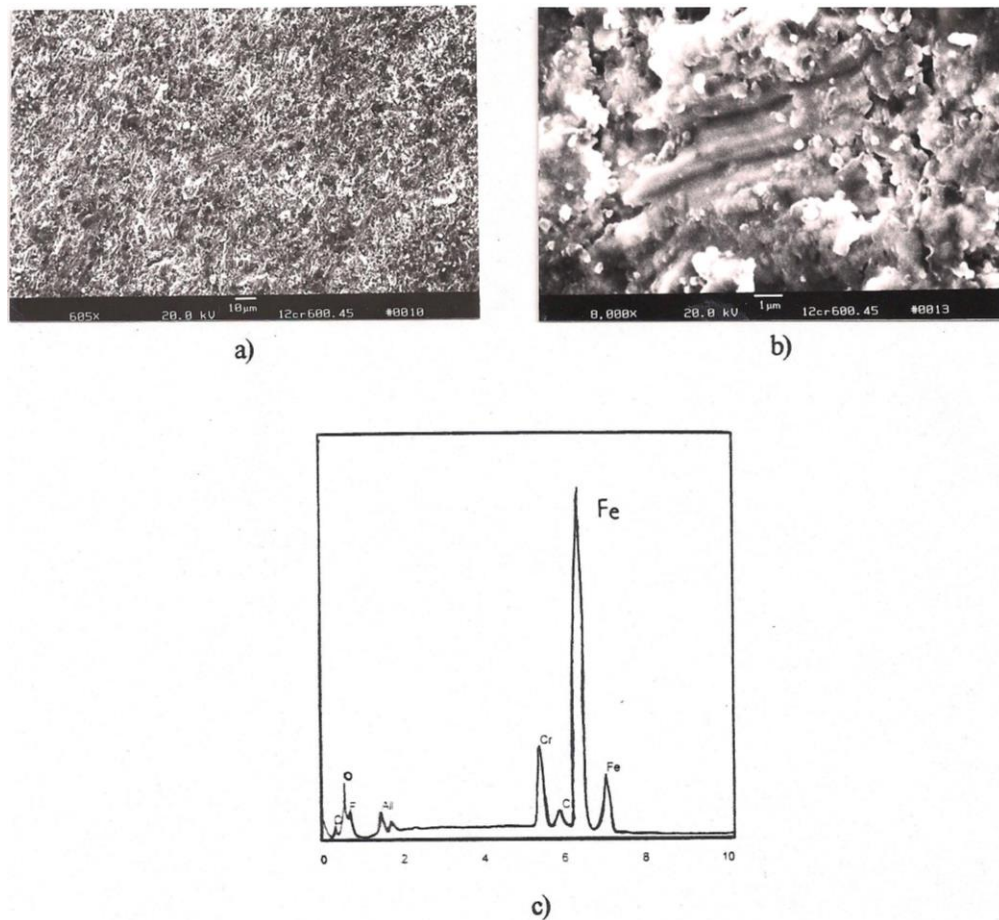


Fig. 6.- SEM micrographs of the 12 Cr SS exposed in the E-C rig at 600°C with the 560 μm alumina particles an impact velocity of 4.5 m/s for 24 h; a) surface morphology, b) detail of a) at higher magnification, and c) EDX analysis of the surface in a).

Effect of Alloy Oxidation Resistance on the Erosion-Corrosion Behaviour.

In this work, the E-C performance of 12 Cr stainless steel was investigated. However, for comparison purposes mild steel (0%wt Cr) was also used. At least in high-temperature oxidizing environments, there is general agreement that, increasing alloy chromium content increases the oxidation resistance, as confirmed in Table II. However, in erosion conditions, the resistance may not show a similar trend. Thus, under the conditions of this work, the behaviour of

these two steels at the various temperatures over the whole velocity range has been correlated with chromium concentration as follows:

Effect at 300°C.

Fig. 7 shows that, at velocities up to 2.0 m/s, small weight gains were recorded for both steels. Above 2 m/s, the following was noted: a) the ranking for the alloy reversed, with mild steel showing higher losses than 12 Cr steel; At higher velocities, i.e. $> 3 \text{ m s}^{-1}$, large increases in weight loss were noted. The results showed that, at this temperature, increasing the chromium content of the steel resulted in a decrease in the erosion-corrosion damage, at least at the highest velocities.

Effect at 450°C.

Here, the results showed that, below 4 m/s, the erosion resistance of mild steel was better than that for the 12 Cr steel, Fig. 8. At higher velocities, the ranking of mild steel and 12 Cr steel was reversed, i.e., the mild steel gave bigger weight losses.

Effect at 600°C.

Fig. 9 shows that below 2.5 m/s the 12 Cr steel gave somewhat bigger weight loss than the mild steel. At impact velocities above 2.5 m/s the ranking of the steels reversed. Also, it should be noted that the velocity at which the ranking of alloys reversed decreased with increasing temperature, see Fig. 8.

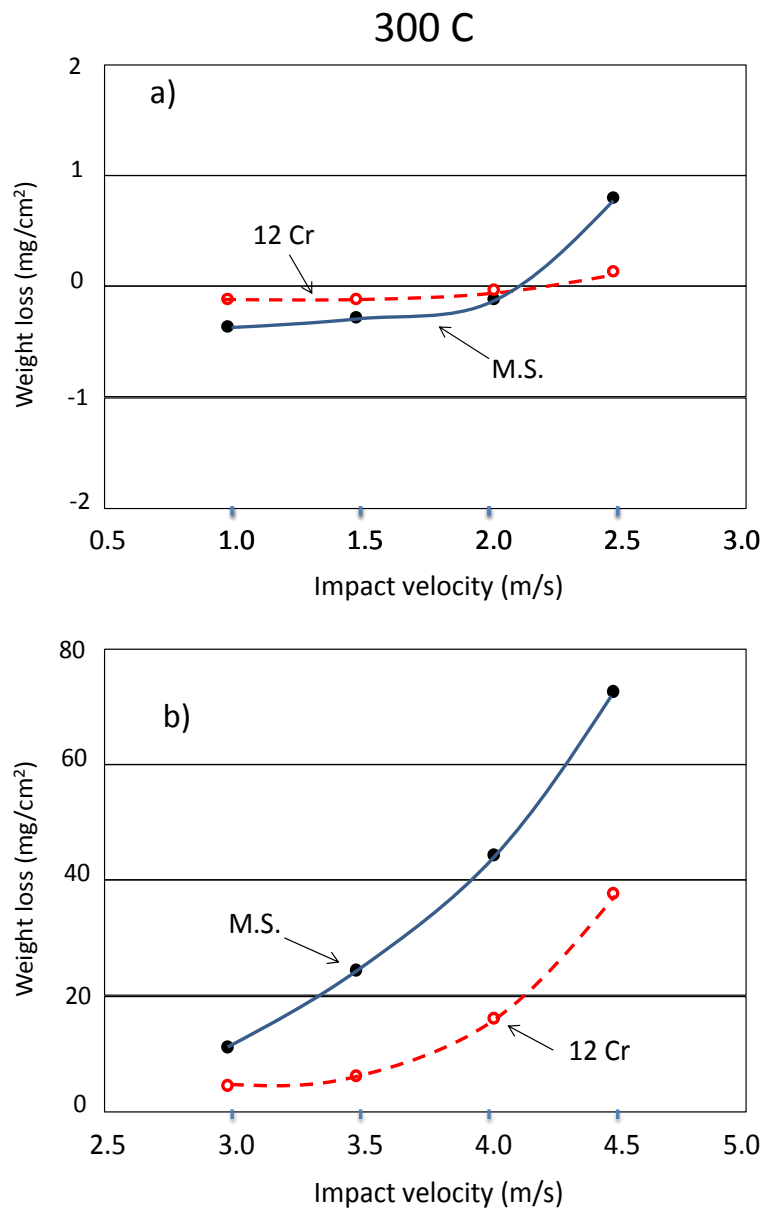


Fig. 7.- Variation of weight loss for 12 Cr SS and mild steel as a function of impact velocity after exposure for 24 h in the E-C rig at 300°C (560 μm alumina particles).

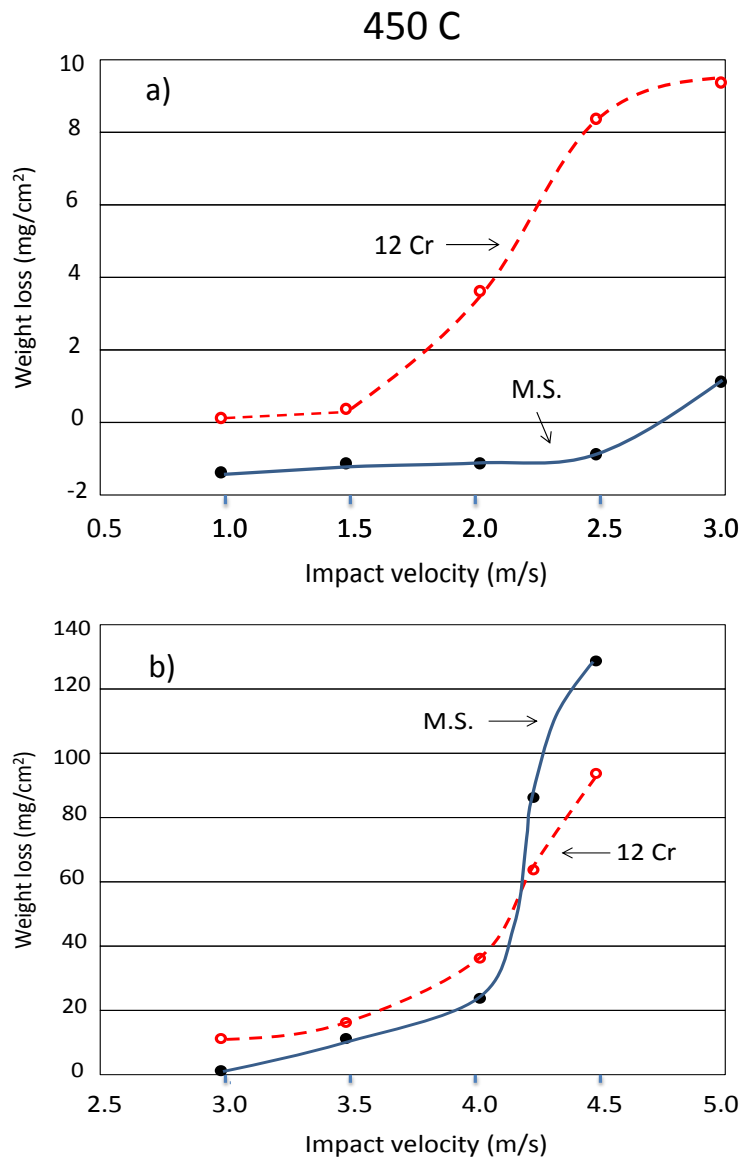


Fig. 8.- Variation of weight loss for 12 Cr SS and mild steel as a function of impact velocity after exposure for 24 h in the E-C rig at 450°C (560 μm alumina particles).

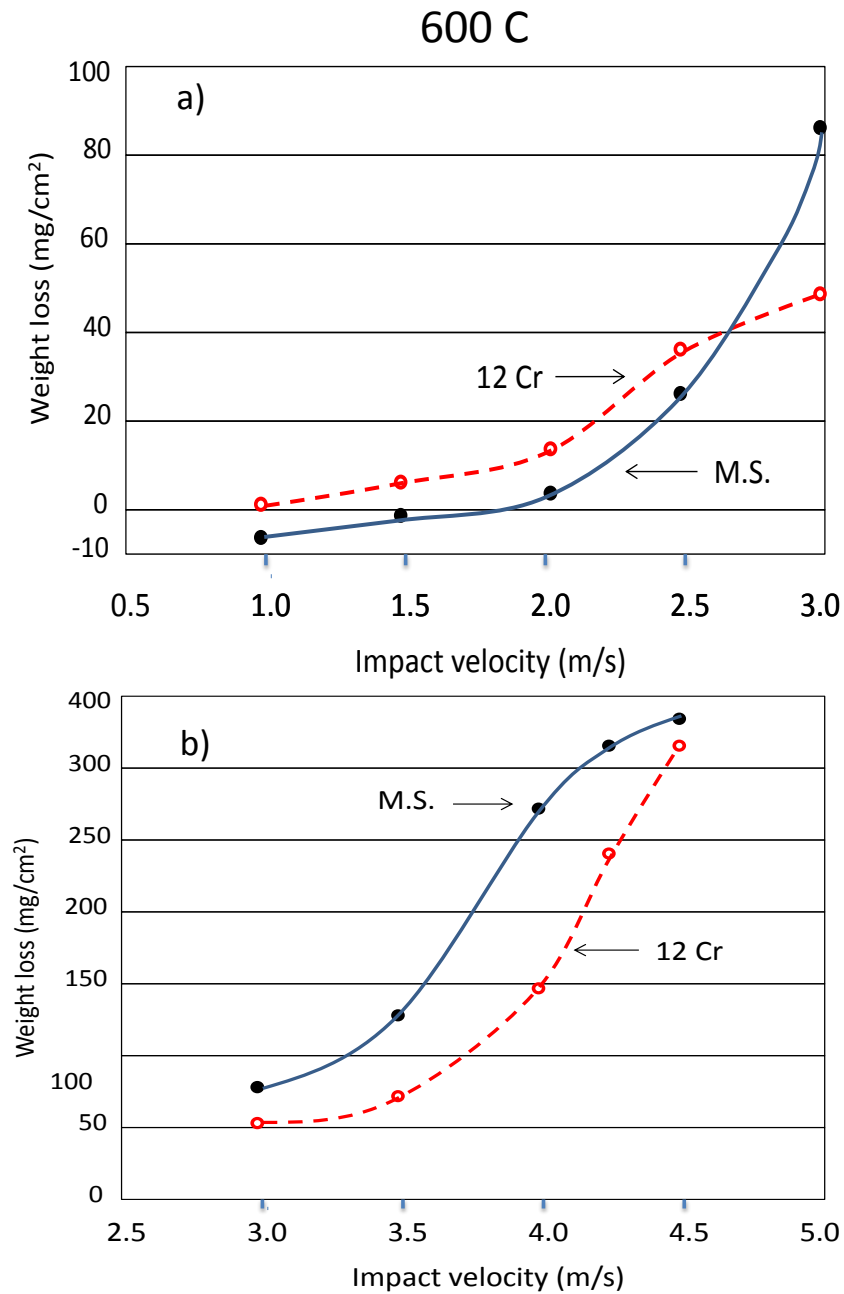


Fig. 9.- Variation of weight loss for 12 Cr SS and mild steel as a function of impact velocity after exposure for 24 h in the E-C rig at 600°C (560 μm alumina particles).

It is interesting to note that at 450⁰C and below an impact velocity of 4 m/s, the wastage for the 12 Cr steel (higher oxidation resistance) was higher than that of the mild steel (lower oxidation resistance). Further, it is interesting to note that, at the highest velocity, the weight losses approached those of mild steel, in both trend and magnitude. Thus, the behavior found indicates that a more oxidation resistant alloy does not necessarily have better resistance under erosion-corrosion conditions.

Weight loss as a function of impact velocity.

Irrespective of the material tested here, the following trends were noted for the velocity range used: at $< 2 \text{ m s}^{-1}$. The weight losses were very small and, sometimes, weight gains were recorded; in the velocity range from 2 m/s to 3.5 m/s the wastage could be represented by either linear or non-linear behaviour; above 3.5 m/s the wastage increased significantly with increases in velocity.

Fig. 10 shows a schematic diagram to indicate the anticipated transitions between the various E-C regimes as a function of impact velocity. Here, a decrease in alloy corrosion rate or an increase in particle erosivity should shift the corrosion-dominated regime to lower velocities. Also, increases in velocity shift the erosion-corrosion behaviour from corrosion dominated to erosion dominated. Last, it is important to point out that increasing the temperature will shift this curve to higher velocities, as the transition to "erosion-dominated" behaviour is achieved at higher velocities.

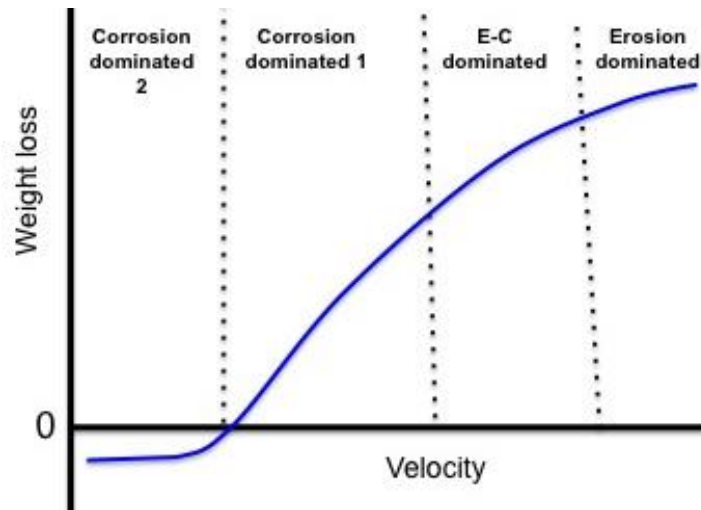


Fig. 10.- Schematic diagram showing the transitions between the E-C regimes as a function of impact velocity.

As an example, we should expect that, above 300⁰C and an impact velocity above of 1 m/s, the 12 Cr steel operates in the erosion-corrosion regime; whereas the mild steel should operate in the corrosion-dominated regime 2 at temperatures above 500⁰C and impact velocities below 2 m/s.

The present results also indicate that the ranking order of erosion-corrosion rates of alloys of different corrosion resistances can reverse in different velocity conditions. Thus, the relative erosion-corrosion resistance of alloys exposed under particular conditions cannot be used arbitrarily to predict wastage rates in other environments, particularly if parameters such as impact velocity are varied significantly.

CONCLUSIONS:

- A study has been carried out on the effects of temperature and impact velocity for 12 Cr steel in elevated temperature laboratory fluidised bed conditions.
- Under the present experimental conditions, the 12 Cr steel did not show a peak wastage temperature. Thus, from the erosion-corrosion regimes defined, the 12 Cr steel operates under the “erosion-corrosion” regime.
- On the whole, the 12 Cr steel gave a poor E-C performance compared with mild steel.
- The ranking order of erosion-corrosion resistance of two alloys of different corrosion resistance can reverse if the velocity is changed significantly.
- The relationship between erosion-corrosion rate and velocity has a significant implication for materials selection in erosion-corrosion environments.

Acknowledgements:

The authors would like to thank Consejo Nacional de Ciencia y Tecnología (CONACyT, Mexico) for the economic support to carry out this work.

References:

- (1) Hou, P., MacAdam, S., Niu, Y. & Stringer, J. (2004). High Temperature Degradation by Erosion-Corrosion in Bubbling Fluidized Bed Combustors. *Materials Research*, Vol.7, No.1, (March 2004), pp. 71-80, ISSN 1516-1439
- (2) Oka, S. (2004). Fluidized Bed Combustion, Marcel Dekker, New York. ISBN 0-8247-4699-6

(3) J. G. Chacon-Nava, F. Almeraya-Calderon, A. Martinez-Villafañe and M. M. Stack, Low Impact Velocity Wastage in FBCs—Experimental Results and Comparison Between Abrasion and Erosion Theories, in Abrasion Resistance of Materials, edited by M. Adamiack, Chapter 5, ISBN 978-953-51-0300-4, 212 pages, publisher: Intech, March 16, 2012.

(4) M. M. Stack, J. G. Chacon-Nava, and F. H. Stott, Sinergism between effects of velocity, temperature, and alloy corrosion resistance in laboratory simulated fluidised bed environments, Mat. Sci. and Tech., Vol. 11, p 1180-1185, November 1995.

(5) N. Gat and W. Tabakoff, Wear, Vol. 5085-92, 1978.

(6) W. A. Pliskin, S. J. Zanin, in Hnd Book of Thin Film Technology, Ed. By L. I. Maissed and R. Glang, Sec. 11-23, McGraw-Hill.

(7) A. J. Ninham, i. M. Hutchings, J. A. Little, Corrosion, Vol. 46, (4) p296-301, 1990.

(8) V.K. Sethi and R.G. Corey, Proc. 7th Int. Conf. on Erosión by Liquid and Solid Impact, Cavendish Lab., Univ. of Cambridge, Cambridge, 1987, paper 73.